MODELLING RECONSTRUCTION QUALITY OF LISSAJOUS UNDERSAMPLED ATOMIC FORCE MICROSCOPY IMAGES

Patrick Steffen Pedersen *Jan Østergaard* *Torben Larsen*

Department of Electronic Systems, Faculty of Engineering and Science, Aalborg University, DK-9220 Aalborg, Denmark

ABSTRACT

The reconstruction quality which can be obtained using compressive sensing depends on a number of elements. In the present paper, we establish performance indicators and use these to model the reconstruction quality of atomic force microscopy images undersampled with Lissajous sampling patterns. For this purpose, we consider previously proposed performance indicators. Furthermore, we propose new performance indicators based on the relative energy of the subsampled dictionary matrix atoms. Through extensive simulations, multiple affine models are evaluated in terms of modified coefficients of determination. The results show that the proposed performance indicators are highly correlated with the average reconstruction quality. In conclusion, the proposed performance indicators can be used to model reconstruction quality for the given application, and the proposed model outperforms the previously established model.

***Index Terms*—** compressive sensing, atomic force microscopy, Lissajous sampling patterns, reconstruction quality

1. INTRODUCTION

Atomic force microscopy (AFM) is an advanced tool for investigating and manipulating nanoscale surfaces [1]. In particular, sub-nanometer resolution 3D surface maps can be obtained when using AFM for high-resolution imaging [2]. This is done by moving the surface and a sharp probe relative to each other whereby a force is asserted on the probe by the surface [3]. Unfortunately, standard AFM image acquisition takes on the order of minutes to hours [4].

One approach to reduce the acquisition time is to reduce the number of samples using compressive sensing (CS) [5]. This recent signal acquisition paradigm allows accurate reconstruction of certain signals from fewer samples than suggested by the Nyquist rate [6]. However, reconstructing the signal means solving a non-convex optimisation problem which, in the noiseless case, takes the form [7]:

$$\begin{aligned} &\text{minimise} && ||\hat{\boldsymbol{\alpha}}||_0 \\ &\text{subject to} && \mathbf{y} = \boldsymbol{\Phi}\boldsymbol{\Psi}\hat{\boldsymbol{\alpha}} \end{aligned} \tag{1}$$

where $\mathbf{y} \in \mathbb{R}^{m\times 1}$ is the sampled vector, $\boldsymbol{\Phi} \in \mathbb{R}^{m\times p}$ is a so-called measurement matrix, $\boldsymbol{\Psi} \in \mathbb{C}^{p\times n}$ is a so-called dictionary matrix, and $\hat{\boldsymbol{\alpha}} \in \mathbb{C}^{n\times 1}$ is the reconstructed coefficent vector. In the present context, $\mathbf{y}$ contains the sampled pixel values, and the reconstructed signal $\boldsymbol{\Psi}\hat{\boldsymbol{\alpha}} = \hat{\mathbf{x}} \in \mathbb{R}^{p\times 1}$ contains the reconstructed pixel values.

In order to acquire an image with AFM using CS, the user must choose $\boldsymbol{\Phi}$ and $\boldsymbol{\Psi}$ in (1) as well as a so-called reconstruction algorithm. In a recent effort, the achievable reconstruction quality is modelled using performance indicators calculated from the $\boldsymbol{\Phi}$ and $\boldsymbol{\Psi}$ [11]. The present paper is concerned with improving the established model for Lissajous measurement matrices and the discrete cosine transform (DCT) dictionary. The Lissajous scanning path has been chosen for its simplicity, ultra-narrow frequency spectrum, low sensitivity to measurement noise, and multiresolution capabilities [1].

In [11], three performance indicators are proposed. The first of these is the well-known quantity of mutual coherence which describes the maximum correlation between the columns of $\boldsymbol{\Psi}$ and the rows of $\boldsymbol{\Phi}$:

$$\mu_{\text{mut}}(\boldsymbol{\Phi}, \boldsymbol{\Psi}) = \max_{1\leq i\leq m, 1\leq j\leq n} |\boldsymbol{\Phi}_{i,:}\boldsymbol{\Psi}_{:,j}|$$

The second performance indicator is the well-known quantity of coherence which describes the maximum correlation between two columns of $\mathbf{A} = \boldsymbol{\Phi}\boldsymbol{\Psi}$:

$$\mu_{\text{coh}}(\boldsymbol{\Phi}, \boldsymbol{\Psi}) = \max_{1\leq i\neq j\leq n} \frac{|\boldsymbol{\Psi}_{:,i}^T\boldsymbol{\Phi}^T\boldsymbol{\Phi}\boldsymbol{\Psi}_{:,j}|}{||\boldsymbol{\Phi}\boldsymbol{\Psi}_{:,i}||_2||\boldsymbol{\Phi}\boldsymbol{\Psi}_{:,j}||_2}$$

Finally, the third performance indicator is the recently established coherence 2-norm which describes the root-mean-square correlation between two columns of $\mathbf{A} = \boldsymbol{\Phi}\boldsymbol{\Psi}$:

$$\mu_{\text{rms}}(\boldsymbol{\Phi}, \boldsymbol{\Psi}) = \sqrt{\frac{1}{n^2-n}\sum_{i=1}^{n}\sum_{\substack{j=1\\ j\neq i}}^{n}\left(\frac{|\boldsymbol{\Psi}_{:,i}^T\boldsymbol{\Phi}^T\boldsymbol{\Phi}\boldsymbol{\Psi}_{:,j}|}{||\boldsymbol{\Phi}\boldsymbol{\Psi}_{:,i}||_2||\boldsymbol{\Phi}\boldsymbol{\Psi}_{:,j}||_2}\right)^2}$$

Based on the above performance indicators, an affine reconstruction quality model was established:

$$\hat{q} = a_1\mu_{\text{mut}} + a_2\mu_{\text{coh}} + a_3\mu_{\text{rel}} + b$$

where the dependency on $\boldsymbol{\Phi}$ and $\boldsymbol{\Psi}$ is implicit.

With the constraints put on $\mathbf{\Phi}$ by the given application, $\mathbf{\Psi}$ is effectively subsampled to form $\mathbf{A} = \mathbf{\Phi\Psi}$. Depending on the subsampling, some active dictionary atoms could have all-zero entries sampled and make reconstruction impossible. To establish a model which accounts for such undesired effects, additional performance indicators are required.

In the present effort, we propose two novel performance indicators to detect incompatibility between $\mathbf{\Phi}$ and $\mathbf{\Psi}$. Based on these and the previously stated performance indicators, we establish a simple affine model to fit the reconstruction quality within CS for AFM constrained to Lissajous sampling patterns and the DCT dictionary. A large number of simulations have been performed to estimate the parameters of the model and evaluate both the model and the performance indicators. The simulations include a number of images, reconstruction algorithms, and measurement matrices. The results show that, in terms of modified R^2, the proposed performance indicators yield better models than the other performance indicators do. Furthermore, the proposed model outperforms the previously established model.

2. INDICATORS

The given application puts certain constraints on $\mathbf{\Phi}$ because AFM physically limits the probe tip to measure only a single point at a time. Thus, each measurement pertains to a single pixel which makes $\mathbf{\Phi}$ extremely sparse. That is, each row of $\mathbf{\Phi}$ only has a single non-zero entry containing the value, one. Furthermore, we do not include the same pixel more than once in $\mathbf{y}$. That is, each column of $\mathbf{\Phi}$ contains at most one non-zero entry. Consequently, $\mathbf{\Psi}$ is effectively subsampled to form $\mathbf{A} = \mathbf{\Phi\Psi}$, and all or most of the non-zero entries of some dictionary atoms could be "missed" in the process.

We propose to determine the extent of the above problem by considering the energy of the subsampled dictionary matrix atoms relative to the energy of the original dictionary matrix atoms:

$$\mathbf{w}(\mathbf{\Phi}, \mathbf{\Psi}) = \begin{bmatrix} \frac{||\mathbf{\Phi\Psi}_{:,1}||_2}{||\mathbf{\Psi}_{:,1}||_2} & \dots & \frac{||\mathbf{\Phi\Psi}_{:,n}||_2}{||\mathbf{\Psi}_{:,n}||_2} \end{bmatrix}^T \tag{2}$$

In order to produce performance indicators, the vector in (2) must be summarised. Based on a number of experiments, the summary statistics chosen are the mean and standard deviation of the relative energies, $\mathbf{w}(\mathbf{\Phi}, \mathbf{\Psi})$:

$$\mu_{\text{rm}}(\mathbf{\Phi}, \mathbf{\Psi}) = \frac{1}{n} \sum_{i=1}^{n} \frac{||\mathbf{\Phi\Psi}_{:,i}||_2}{||\mathbf{\Psi}_{:,i}||_2}$$

$$\mu_{\text{rs}}(\mathbf{\Phi}, \mathbf{\Psi}) = \sqrt{\frac{1}{n} \sum_{i=1}^{n} \left(\frac{||\mathbf{\Phi\Psi}_{:,i}||_2}{||\mathbf{\Psi}_{:,i}||_2} - \mu_{\text{rm}}(\mathbf{\Phi}, \mathbf{\Psi}) \right)^2}$$

3. SIMULATIONS

In order to model reconstruction quality, the model must be established and its parameters must be estimated. Therefore, we have performed an experiment for each combination across a set of images, a set of sampling patterns, and a set of reconstruction algorithms. Each experiment consists of solving the reconstruction problem, computing the reconstruction quality, and calculating the values of the set of performance indicators.

The set of images consists of seven images of biological cells. These images have been acquired with a resolution of 512×512 pixels on Keysight Technologies ILM6000 and ILM7500 AFM equipment. Using a square matrix for dictionary matrix, this resolution results in $\mathbf{\Psi} \in \mathbb{C}^{512^2 \times 512^2}$ which takes up $1\,\text{TiB}$ of memory, when represented with $64\,\text{bit}$ floats. To make the involved computations feasible, the images have been subsequently down-sampled to 128×128 pixels.

The sampling patterns are based on Lissajous-shaped scanning paths [1]. The Lissajous-shaped scanning paths can be defined by the $x(t)$ and $y(t)$ coordinates for t in some range:

$$x(t) = c_x \sin(2\pi f_x t + \theta_x) \quad , \quad y(t) = c_y \sin(2\pi f_y t + \theta_y)$$

where c_x and c_y are given by the dimensions of the scanned area, f_x and f_y are the frequencies, and θ_x and θ_y are the initial phases. The set of sampling patterns consists of matrix representations of these scanning paths using varying parameters and undersampling ratios, δ:

$$\begin{aligned} f_x &\in \{5 + i | i = 0, \dots, 10\} \\ f_y &\in \{5 + i | i = 0, \dots, 10\} \\ \theta_x &\in \left\{ \frac{i}{8}\pi \middle| i = 0, \dots, 4 \right\} \\ \theta_y &\in \left\{ \frac{1}{2}\pi + \frac{i}{8}\pi \middle| i = 0, \dots, 4 \right\} \\ \delta &\in \{0.1 + i \cdot 0.025 | i = 0, \dots, 8\} \end{aligned}$$

The set of reconstruction algorithms consists of the iterative soft thresholding (IST) algorithm [8] and an ℓ_1-minimisation algorithm [9]. Finally, the set of performance indicators consists of the performance indicators presented in Section 1 and 2.

Before the actual reconstruction is performed, the image of interest is sampled by applying the measurement matrix and detilted by least-squares-fitting a plane and subtracting this. The same plane is subtracted from the original image before the reconstruction quality is computed. For most of the actual implementation, the Magni software package [10] is used. Furthermore, the PyUNLocBoX software package[1]

[1] Available at https://github.com/epfl-lts2/pyunlocbox.

is used for its implementation of the ℓ_1-minimisation image reconstruction using Douglas-Rachford splitting. Finally, the peak signal-to-noise-ratio (PSNR) metric is used to asses the reconstruction quality, with the peak value, P, being the maximum possible pixel value:

$$\text{PSNR} = 10\log_{10}\left(\frac{P^2}{||\mathbf{x}-\hat{\mathbf{x}}||_2^2}\right)$$

Based on the results, as presented in Section 4, and for comparability with [11], we have chosen to model the reconstruction quality affinely in terms of the performance indicators. That is,

$$\hat{q}_i = \sum_k (a_k c_{k,i}) + b \tag{3}$$

where $\hat{q}_i$ is the predicted reconstruction quality for the i^{th} measurement matrix, a_k is the coefficient of the k^{th} performance indicator, $c_{k,i}$ is the value of the k^{th} performance indicator for the i^{th} measurement matrix, and b is an offset.

The coefficients are estimated using a least-squares-fit, and, in order to evaluate the usefulness of the established model, the modified coefficient of determination, $\tilde{R}^2$, is used [11]:

$$\tilde{R}^2 = 1 - \frac{\sum_{i=1}^{s}(\bar{q}_i - \hat{q}_i)^2}{\sum_{i=1}^{s}(\bar{q}_i - \bar{q})^2}$$

$$\bar{q}_i = \frac{1}{t_i}\sum_{j=1}^{t_i} q_{ij} \quad , \quad \bar{q} = \frac{1}{s}\sum_{i=1}^{s}\bar{q}_i$$

where q_{ij} is the reconstruction quality for the i^{th} measurement matrix for the j^{th} combination of image and reconstruction algorithm, s is the number of measurement matrices, and t_i is the number of combinations of images and reconstruction algorithms for the i^{th} measurement matrix.

4. RESULTS

Using the simulated set of data, three models of the form given by (3) were analysed: 1) one baseline model using the mutual coherence, the coherence 2-norm, and the coherence as proposed in [11], 2) one model using only the relative-energy-mean, and 3) one proposed model using the coherence, the relative-energy-mean, and the relative-energy-standard-deviation. Table 1 lists the resulting parameters along with the $\tilde{R}^2$ value for each model.

The simulated set of data is visualised in three subplots in Figure 1: the figure shows the obtained reconstruction qualities, q_{ij}, and the average reconstruction qualities, $\bar{q}_i$, plotted against the reconstruction qualities predicted by each of the three models, respectively.

Table 1. Model parameters and evaluation.

Model	a_{mut}	a_{rms}	a_{coh}	a_{rm}	a_{rs}	b	$\tilde{R}^2$
base	0.47	-141	-12.3	-	-	29.9	0.89
rm	-	-	-	29	-	8.1	0.94
prop	-	-	-5.6	18	317	12.0	0.96

5. DISCUSSION

Clearly, the relative-energy-mean is a good indicator of the performance in terms of reconstruction quality. Impressively, the rm model based solely on this performance indicator accounts for roughly $95\,\%$ of the variation in average reconstruction quality and thereby outperforms the baseline model which uses three performance indicators established in [11]. We offer the interpretation that the sampling pattern should be chosen such that it preserves as much energy of the dictionary matrix as possible. According to the rm model, the maximum achievable average reconstruction quality is approximately $37\,\text{dB}$, since the relative-energy-mean cannot exceed the value, 1, given the constraints on $\mathbf{\Phi}$ explained in Section 2.

Interestingly, in the proposed model, the a_{rs} value is positive and more than one order of magnitude larger than a_{rm}. That is, the reconstruction quality should increase if the relative-energy-mean is decreased as long as the relative-energy-standard-deviation is increased slightly. Such behaviour would violate the intuition motivated in the previous paragraph. However, we suggest that the model merely promotes larger relative energies, and that larger relative energies result in increases in both mean and standard deviation. This suggestion is supported by the close-to-one modified coefficient of determination of the model relying solely on the relative-energy-mean.

The baseline model is able to account for roughly $90\,\%$ of the variation in average reconstruction quality, which supports the usefulness of the performance indicators established in [11]. The changes in the model coefficient values and the increase in modified coefficent of determination are attributed to the fact that fewer sampling pattern families, fewer dictionaries, and fewer reconstruction algorithms were used for the simulations of the present effort.

6. CONCLUSIONS AND FUTURE WORK

The purpose of the present paper is to model reconstruction quality from performance indicators, which are properties of the measurement matrix and the dictionary matrix. We have proposed the relative-energy-mean performance indicator which can account for roughly $95\,\%$ of the observed variation in average reconstruction quality. The results show that even more of this variation can be accounted for using an affine model based on the relative-energy-mean performance indi-

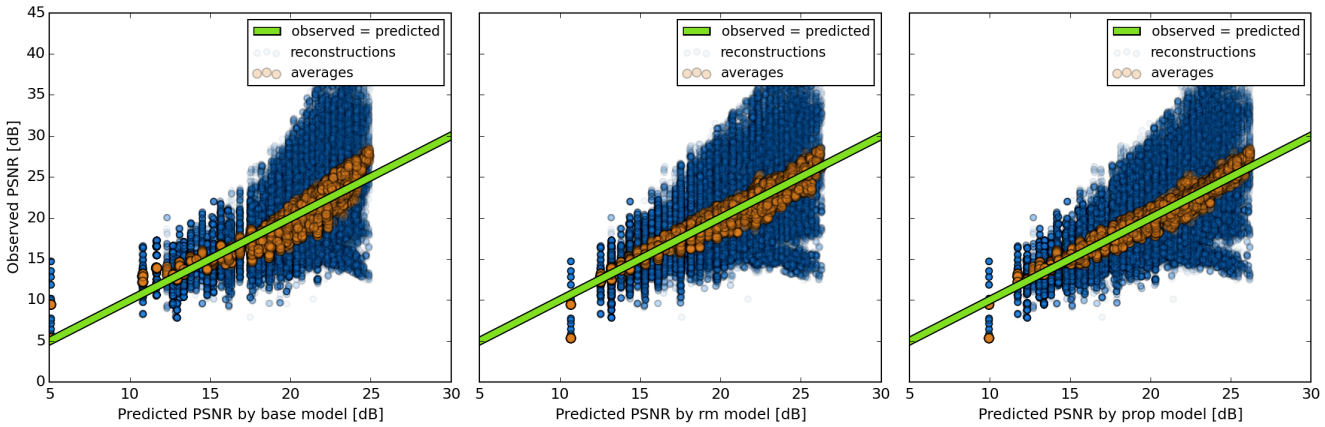

Fig. 1. The obtained PSNR values, q_{ij}, and the average obtained PSNR values, $\bar{q}_i$, versus the PSNR values predicted by the three models, respectively.

cator, the well-known coherence quantity, and the proposed relative-energy-standard-deviation performance indicator.

In the present paper, the proposed performance indicators have been used for improving an existing model of the reconstruction quality which can be obtained in CS problems within AFM. However, it has been suggested that performance indicators could be used for optimising measurement matrices and/or dictionary matrices. With the improvements in terms of the modified coefficient of determination, the proposed performance indicators should be even better suited for this application. Thus, potentially, the proposed relative energy performance indicators could contribute to new learning algorithms for CS or improve existing ones.

7. REFERENCES

[1] T. Tuma, J. Lygeros, V. Kartik, A. Sebastian, and A. Pantazi, "High-speed multiresolution scanning probe microscopy based on Lissajous scan trajectories," *Nanotechnology*, vol. 23, no. 18, pp. 9, Apr. 2012.

[2] D. Y. Abramovitch, S. B. Andersson, L. Y. Pao, and G. Schitter, "A Tutorial on the Mechanisms, Dynamics, and Control of Atomic Force Microscopes," in *American Control Conference*, New York City, USA, July 11-13, 2007, pp. 3488–3502.

[3] B. Bhushan and O. Marti, "Scanning Probe Microscopy – Principle of Operation, Instrumentation, and Probes," in *Springer Handbook of Nanotechnology*, Bharat Bhushan, Ed., chapter 21, pp. 573–617. Springer Berlin Heidelberg, 2010.

[4] Y. K. Yong, A. Bazaei, S. O. R. Moheimani, and F. Allgöwer, "Design and Control of a Novel Non-Raster Scan Pattern for Fast Scanning Probe Microscopy," in *IEEE/ASME International Conference on Advanced Intelligent Mechatronics (AIM)*, Kachsiung, Taiwan, July, 11 – 14, 2012, pp. 456–461.

[5] S. B. Andersson and L. Y. Pao, "Non-Raster Sampling in Atomic Force Microscopy: A Compressed Sensing Approach," in *American Control Conference (ACC)*, Montréal, Canada, June 27-29, 2012, pp. 2485–2490.

[6] J. Romberg, "Imaging via Compressive Sampling," *IEEE Signal Processing Magazine*, vol. 25, no. 2, pp. 14–20, Mar. 2008.

[7] E. J. Candès, J. Romberg, and T. Tao, "Robust Uncertainty Principles: Exact Signal Reconstruction From Highly Incomplete Frequency Information," *IEEE Transactions on Information Theory*, vol. 52, no. 2, pp. 489–509, Feb. 2006.

[8] I. Daubechies, M. Defrise, and C. De Mol, "An Iterative Thresholding Algorithm for Linear Inverse Problems with a Sparsity Constraint," *Communications on Pure and Applied Mathematics*, vol. 57, no. 11, pp. 1413–1457, Nov. 2004.

[9] D. L. Donoho, "Compressed Sensing," *IEEE Transactions on Information Theory*, vol. 52, no. 4, pp. 1289–1306, Apr. 2006.

[10] C. S. Oxvig, P. S. Pedersen, T. Arildsen, J. Østergaard, and T. Larsen, "Magni: A Python Package for Compressive Sampling and Reconstruction of Atomic Force Microscopy Images," *Journal of Open Research Software*, vol. 2, no. 1, pp. e29, Oct. 2014.

[11] P. S. Pedersen, J. Østergaard, and T. Larsen, "Predicting Reconstruction Quality Within Compressive Sensing for Atomic Force Microscopy," *IEEE Global Conference on Signal and Information Processing*, Orlando, USA, December 14-16, 2015, accepted.